SARL au capital de 50 000 Euros
10 impasse Borde-basse Z. A. La Violette, 31240 L'Union France
RCS Toulouse B 389 259 706 SIRET 389 259 709 00031
VAT FR10 389 259 706 APE 7490B
TEL 33 (0)5 61 09 47 45 FAX 33 (0)5 61 74 62 22
E-mail: info@interac.fr www.interac.fr

Ingénierie Technique & Recherche en Acoustique
Technical Engineering & Research in Acoustics

Technical Report

Force identification of Shock Machine

Test campaigns in FCBA

for Silent Timber Build project

Author: Dr. Gérard Borello

Date: 2015-10-26

InterAC reference: RT15B158-Rev1-Shock Machine

Abbreviations

ESEA	Experimental Statistical Energy Analysis
DLF	Damping Loss Factor(s)
FRF	Frequency Response Function
HF	High Frequency
LF	Low Frequency
LMPR	Local Modal Phase Reconstruction
PIM	Power Injected Method
PSD	Power Spectral Density
rms	root mean squared value
SEA	Statistical Energy Analysis

Contents

List of Figures

1. Introduction

This report describes experimental investigations and related post-processing for identifying mechanical forces exerted by a typical shock machine on a floor. The identified forces are intended to feed input of a further theoretical SEA model of a building in order to predict noise annoyance resulting from such a source.

2. First test campaign in FCBA

The tests were performed in FCBA on March, 2015 in FCBA facilities.

2.1 Test conditions

2.1.1 Shock machine

The shock machine used as exciter during the testing is the Bruel&Kjaer machine type 3207 equipped with five hammers as shown in next picture.

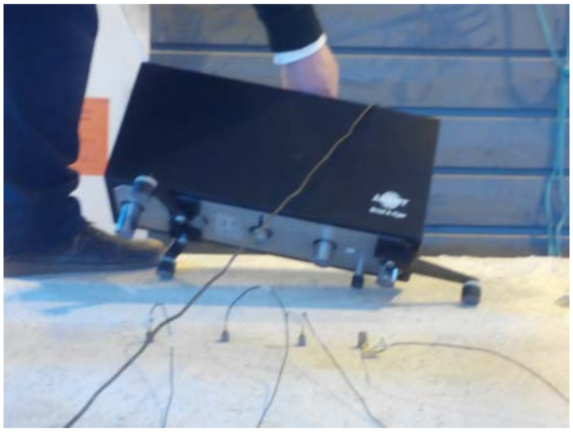

Figure 1: B&K shock machine used as exciter

2.1.2 Impact hammers

Two impact hammers equipped with force cells are used for injecting a known vibrational power in the floors. The first one is a mid-sized Kistler hammer for mid and high frequencies (InterAC equipment) and the second a Dytran large-sized hammer (FCBA equipment) for exciting low frequencies. The Kistler hammer is seen in next picture.

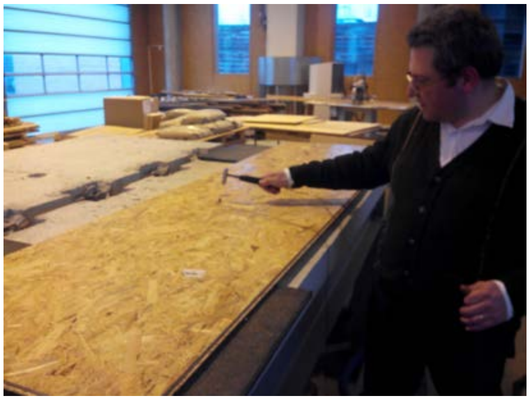

Figure 2: Operating power injection measurement with the Kistler hammer

2.1.3 Transducers

When actuating impact hammers, force is recorded thanks to their built-in force transducer. Acceleration is recorded at various points on floors using different types of ICP accelerometers: one Kistler 50 mV/g, three B&K 100 mV/g and one B&K 10 mV/g.

2.2 Tested floors

A first series of test is performed on a concrete floor (typically 1 m x 6 m flat piece of 9com concrete supported by metallic I-beams). The concrete floor is seen in next picture.

Figure 3: Concrete floor with accelerometer and shock machine in extreme right position

A second series of test is performed on a flat panel of OSB18 supported on two resilient layers and installed on previous concrete floor.

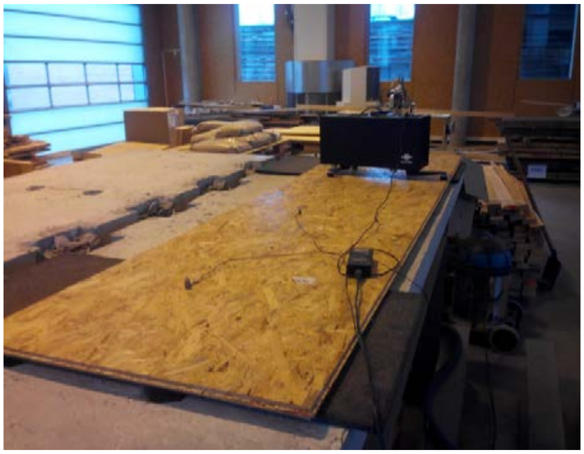

Figure 4: OSB 18 panel mounted on resilient layers and shock machine in extreme right position

2.3 Test sequences

2.3.1 Acquisition system

Data are acquired by a National Instruments 4-channel USB board connected to a note book and driven by SEA-XP 2014 acquisition software from InterAC, dedicated to experimental SEA measurements.

Transfer functions and time histories under impact hammer excitation are recorded as time windows of 4k-samples at 50 kHz rate.

Time histories under shock machine excitation are recorded as time windows of 32k-samples at 25 kHz rate.

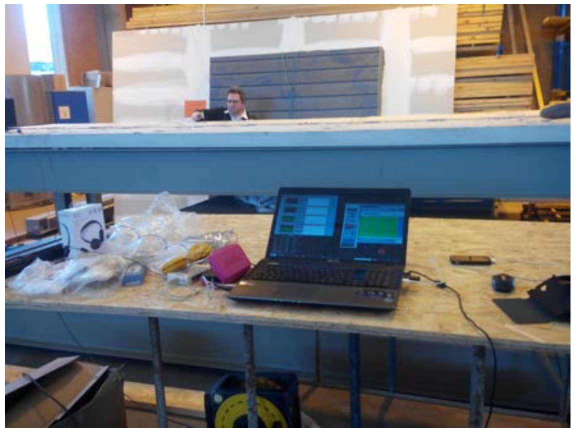

Figure 5: Notebook and card driven by SEA-XP software

2.3.2 Concrete floor test sequences

The concrete floor behavior is first investigated by measuring transfer frequency responses functions under impact hammer. The aim is to estimate the damping loss factor (DLF) of the concrete floor, its driving point mobility and mean transfer squared velocity under this controlled input. Because the concrete floor is very stiff, the two impact hammers are successively used , the large hammer giving better noise/signal ratio in LF range (but with cut-off frequency around kHz) while the mid-sized hammer is providing response ranging between 500 Hz up to 3000 Hz.

Second the shock machine is put in position on the floor at four different locations with fixed four transducers positioned in the middle of the concrete floor

Figure 6: The four fixed location accelerometers used when shock machine is put on floor

2.3.3 OSB floor test sequences

Same sequences are reiterated for the OSB floor, while skipping the large hammer sequence as noise ratio is always good enough with mid-sized hammer on this light-weighted floor.

Figure 7: OSB floor under hammering with mid-sized hammer

2.4 Post-processing analysis: Concrete floor analysis

2.4.1 Analyzing response under mid-sized and large-sized impact hammers

SEA-XP software is used to generate SEA parameters from previous measurements. SEA-XP provides:

- The conductance *Y* (injected power/unit force) computed in frequency domain as real part of mean FRF V/F at driving point
- The mean squared transfer velocity $< v^2 >$ computed in frequency domain from modulus $|V/F|^2$ averaged over various locations of accelerometer and hammer impact over the floor domain
- The mean reverberation time in the floor (computed from FRF impulse response) and transformed into apparent DLF and equivalent mass
- From previous data, the experimental SEA model of the floor (1-subsystem model) is generated and solved. On output, it gives a DLF computed as: $\eta(\omega) = \dfrac{Y}{\omega m \langle v^2 \rangle}$

The two hammers show different validity bandwidth: large-sized hammer gives a correct response up to 800 Hz and the mid-sized hammer up to 2500 Hz.

Between 100 and 800 Hz, data from large and mid-hammers are geometrically averaged as both measurements are valid but still depending on location due low modal density of the concrete floor.

Below 100 Hz only large hammer data are retained and symmetrically above 800 Hz only mid-hammer data are retained.

Measured and averaged conductances spectra are given in 1/3rd octave bands in Figure 8.

DLF averaged over LH and MH tests is given in Figure 11. DLF is around 10% at 100 Hz and shows a decaying slope (5% value at 1000 Hz).

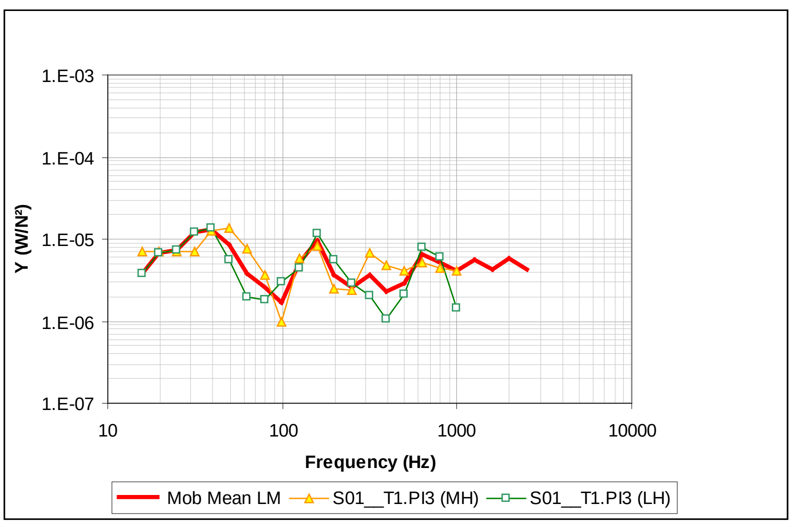

Figure 8: Conductance measured at driving points with large (LH) and mid-hammers (MH) and averaged

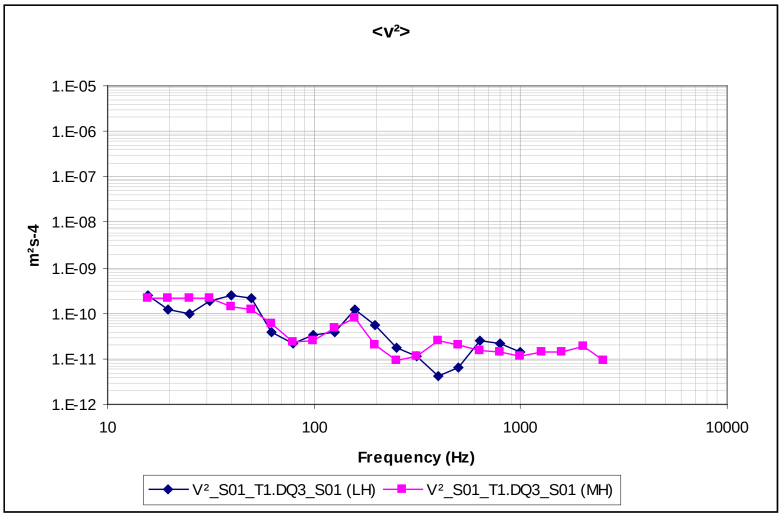

Figure 9: Mean squared velocity of the floor under impact measurement with large and mid-hammers

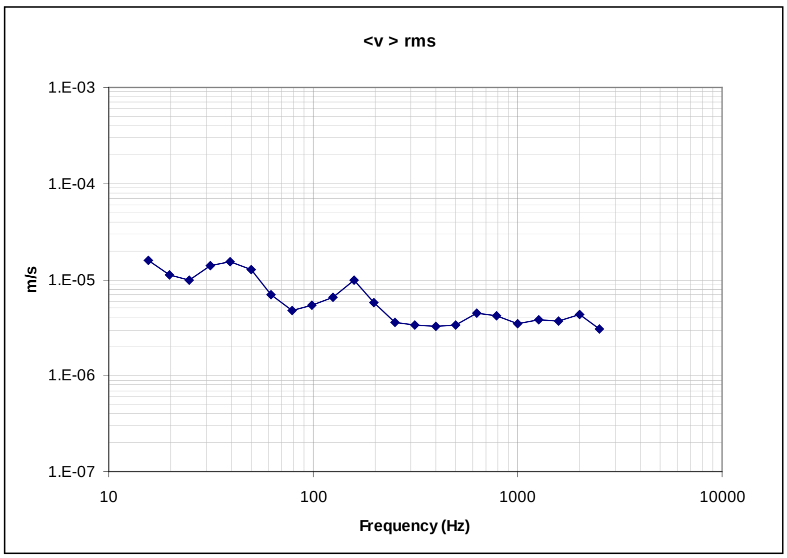

Figure 10: Mean rms velocity of the floor averaged over LH and MH results

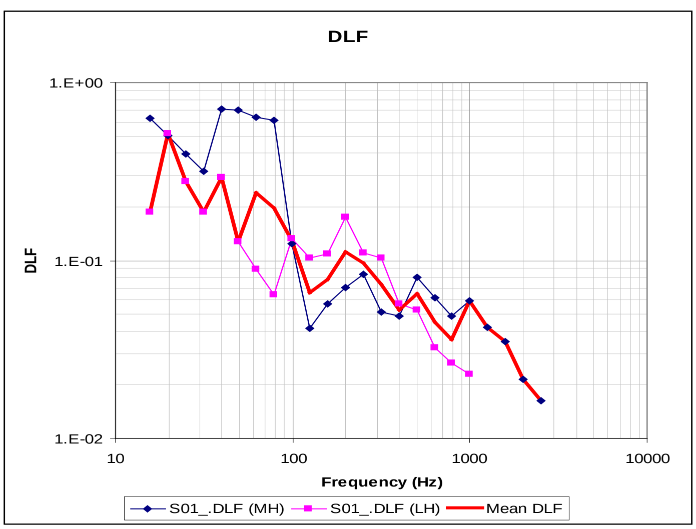

Figure 11: Mean damping loss factor (DLF) of the concrete floor averaged over LH and MH tests

2.4.2 Analyzing response under B&K shock machine

The shock machine response is recorded for 4 positions of the shock machine. Peak time histories are dropping by a factor of 3 between position 1 and 4.

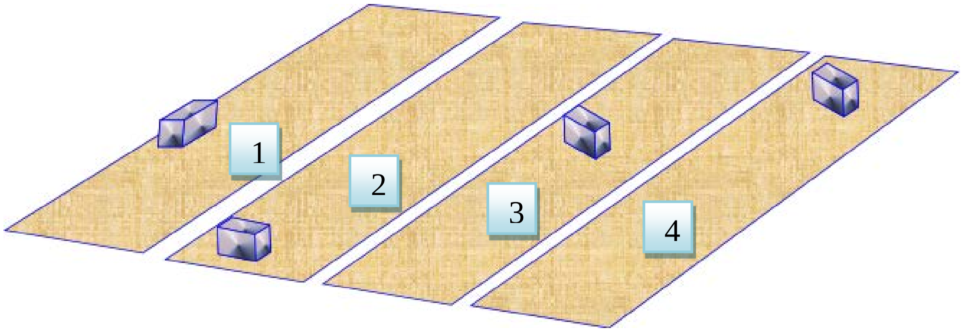

Figure 12: Shock machine in last position and the four accelerometers at fixed location

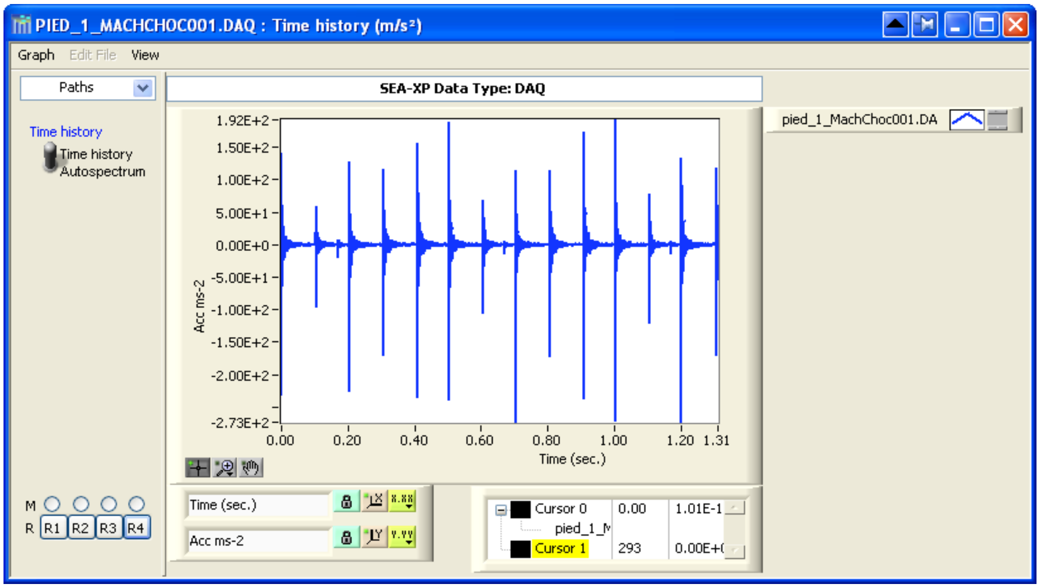

Figure 13: Acceleration time history of first accelerometer in nearest position from shock machine (about 20 cm)

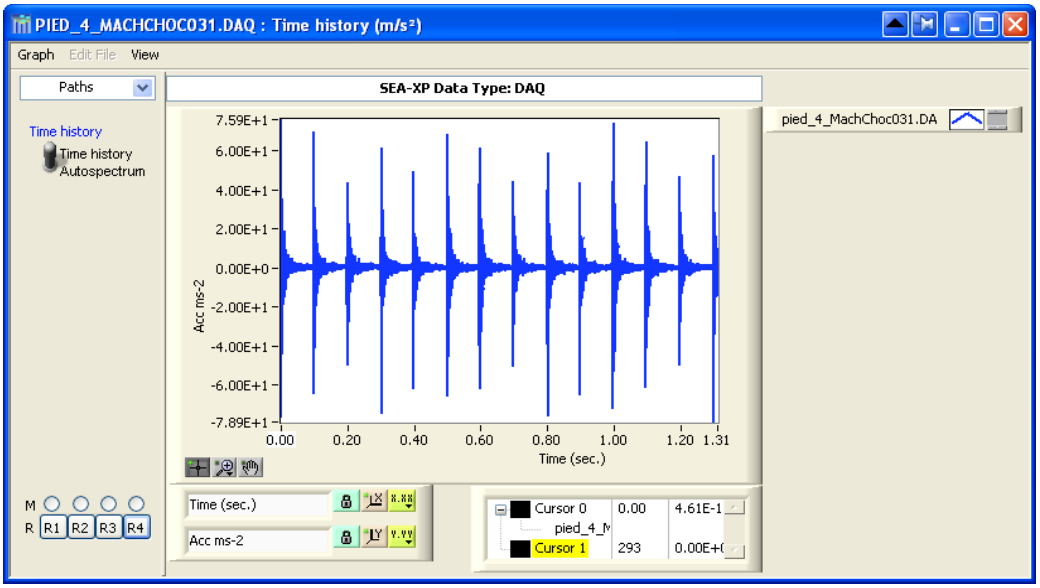

Figure 14: Acceleration time history of first accelerometer in furthest position from shock machine (about 20 cm)

The mean autospectrum S_{vv} is computed in narrow band from all recorded time histories and for all positions and given in Figure 15.

The mean rms velocity of the concrete floor to the shock machine excitation is computed as:

$$\left\langle v^2(f,\Delta f\right\rangle = \sqrt{\frac{1}{\omega_c^2}\int_{\Delta f} S_{vv}(f)df}$$

Related spectrum is given in Figure 16.

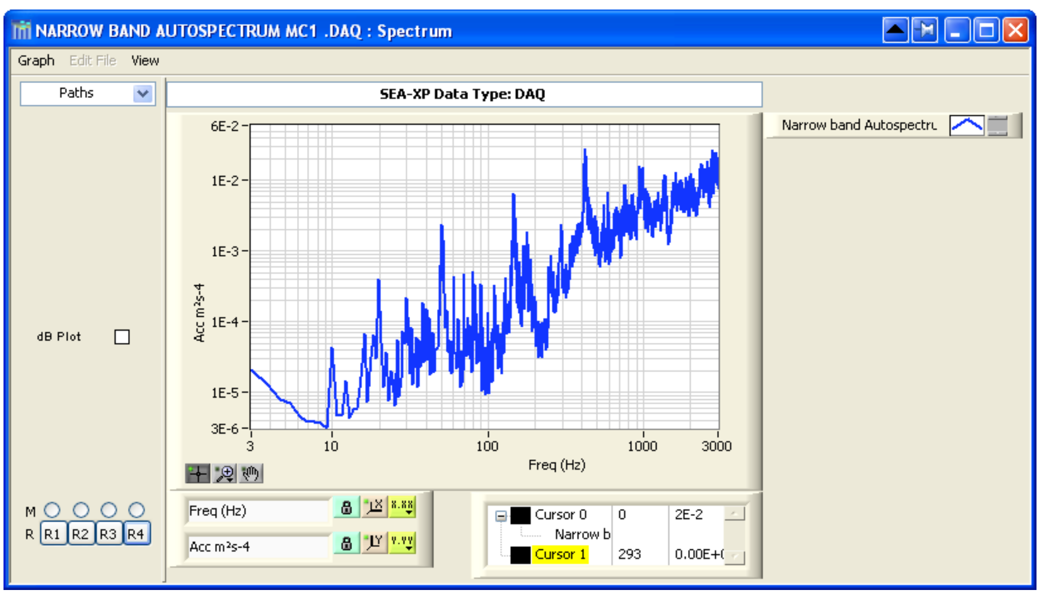

Figure 15: Autospectrum of the mean acceleration response to shock machine computed from all recorded time histories

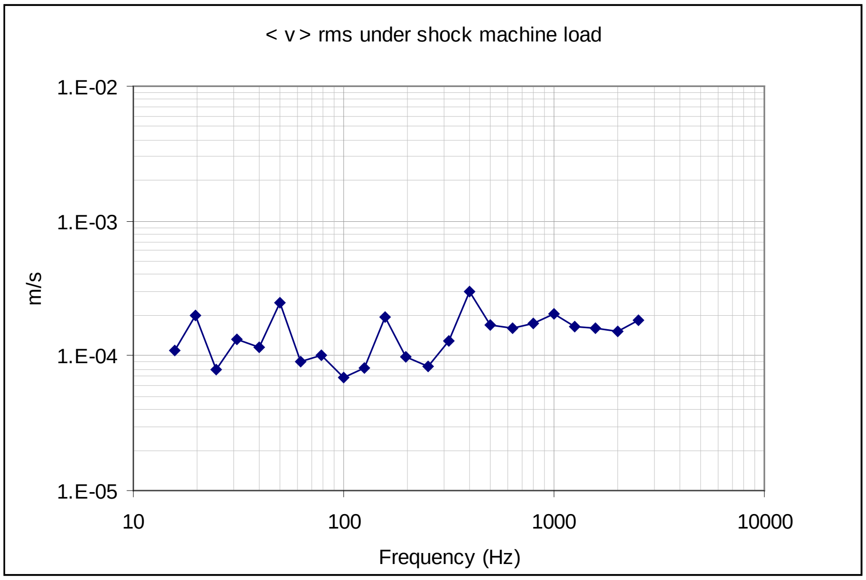

Figure 16: Mean velocity rms response of the concrete floor to shock machine (in 1/3rd octave band

2.4.3 Equivalent force exerted by shock machine on the concrete floor

To extrapolate the force exerted by the shock machine, the transfer $H_1 = \langle v^2 \rangle_1 / Y_1$ is first estimated from impact hammer tests in which *Y* (the driving point mobility) was measured.

In the shock test, it is assumed same function applies as impact from individual shock machine hammers are not too different from the one that was used in impact tests.Then,

$$H_1 = \langle v^2 \rangle_2 / P_2 \Rightarrow P_2 = \langle v^2 \rangle_2 / H_1$$

where P_2 is the total injected power by the shock machine and $\langle v^2 \rangle_2$ the mean response of the concrete floor in term of squared velocity. The rms spectrum of the force is then obtained from:

$$F = \sqrt{P_2 / Y_1}$$

because time histories of the shock machine hammer are well separated in time and they not interfere. The rms force spectrum calculated by this mean is given in Figure 17.

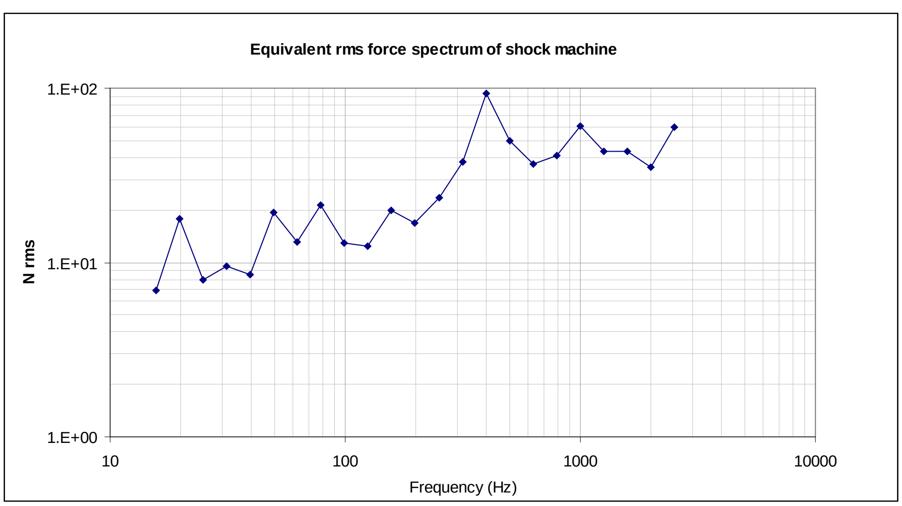

Figure 17: Equivalent rms force from the shock machine on the concrete floor (in 1/3rd octave band)

2.4.4 Validation of force identification

To validate previous post-processing, a SEA theoretical model of the floor is built. The model is thus checked against experimental SEA results where all parameters are under control. The measured SEA DLF is allocated to the floor subsystem which is excited by the measured mean injected power identified under impact hammer. Elastic characteristics of the concrete material are slightly adjusted from default values for improving correlation with conductance measurements. E is decreased from 1E11 down to 8E11. Mass density is kept at default (2300 Kg/m^3).

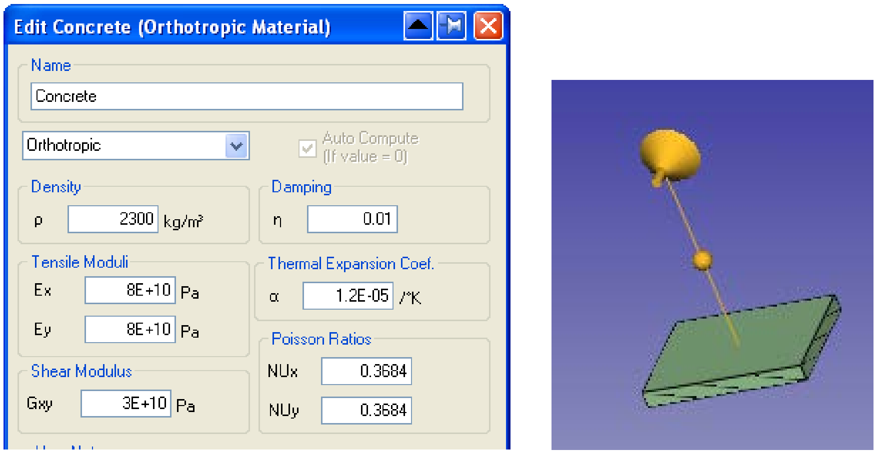

Figure 18: SEA+ floor model for correlation with impact hammer tests

Corresponding SEA model of the floor is very simple, just one plate subsystem in concrete 90mm with dimensions 1m x 6 m excited by the user-defined measured mean power.

The calculated conductance (or shortly the mobility) is compared with measured mean value Y and excellent agreement is found above the first mode of the floor which cannot be predicted accurately by the analytical SEA model. The prediction of mean rms velocity response is compared with measured velocity in Figure 20 where agreement is found excellent up to max frequency of the measurement (3000 Hz).

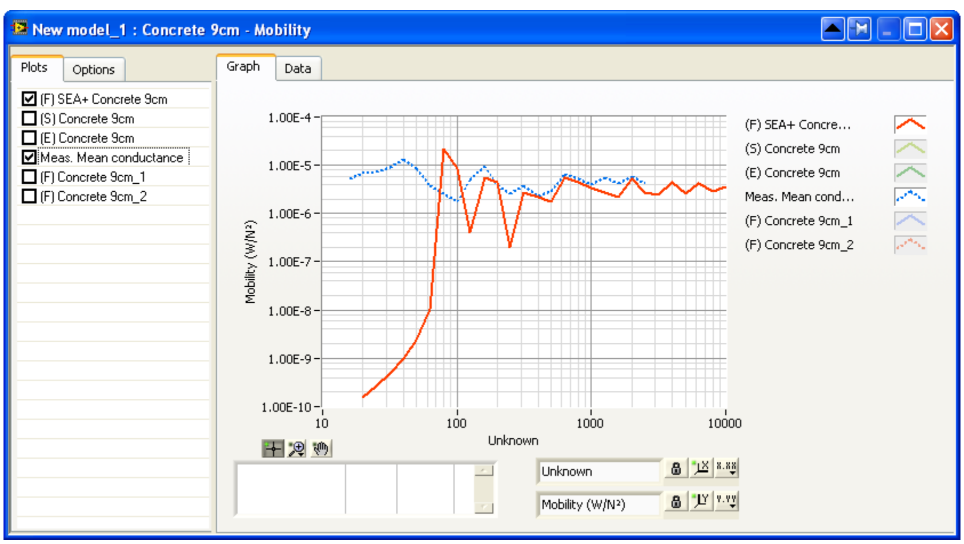

Figure 19: Conductances measured and predicted by the concrete floor SEA+ model

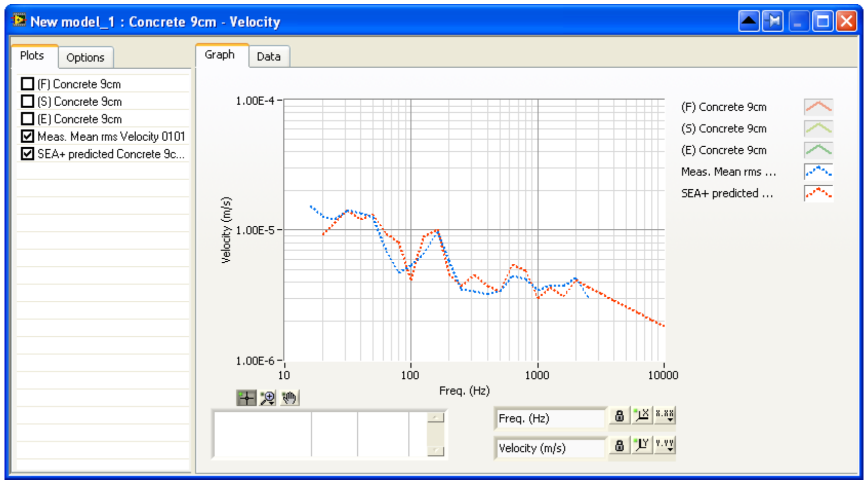

Figure 20: Mean rms velocity responses of the concrete floor measured and predicted by the concrete floor SEA+ model under measured injected power from impact hammer

A second model is then built by simply applying to the same concrete floor subsystem the previously identified force from the shock machine. The SEA+ model is now predicting the mean velocity response compared with measurement in Figure 22. The excellent agreement above 40 Hz is validating our initial assumption that the shock machine is acting not very differently from an impact hammer.

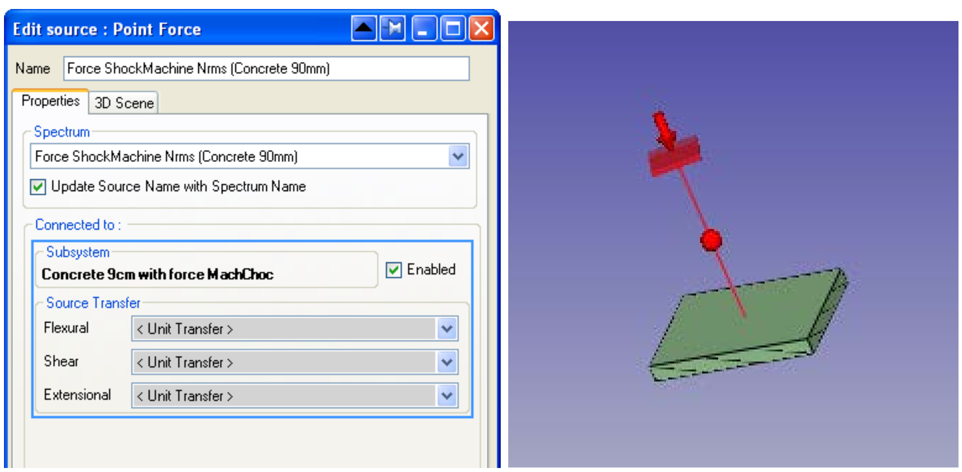

Figure 21: Applying the equivalent force of the shock machine as a point force to the concrete floor

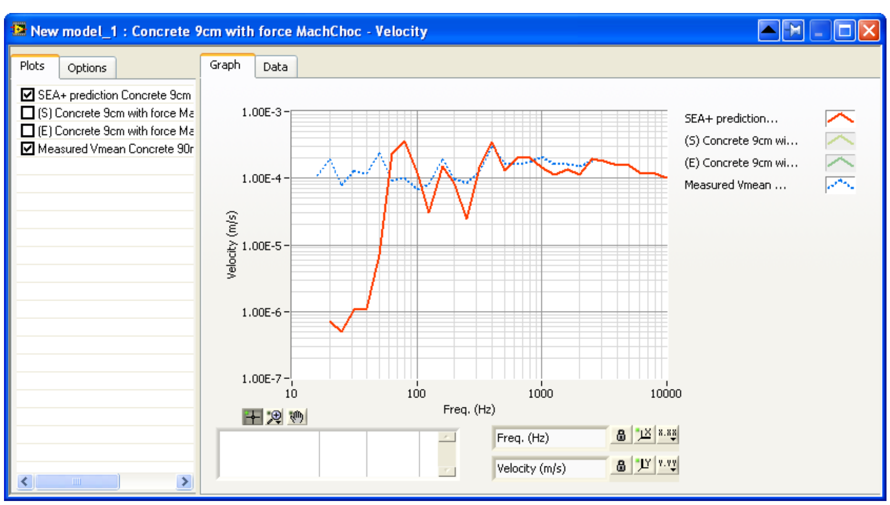

Figure 22: Mean rms velocity responses of the concrete floor measured and predicted by the concrete floor SEA+ model under shock machine equivalent force

2.5 Post-processing data: OSB18 floor analysis

2.5.1 Measurement analysis

The post-processing is similar to Concrete case: PIM method is applied to identify conductance, DLF and equivalent mass of the subsystem under impact hammer. The conductance is given in Figure 23 for the region where OSB panel is freely moving and in the region where it is supported by the resilient layer. Slightly lower conductance is found in the latter case at low frequencies while it becomes slightly larger than free conductance at high frequencies which may be due to accelerometer mounting or to effective additional HF resonance of OSB on top of resilient layer.

The experimental DLF and the related equivalent mass are given in Figure 24.

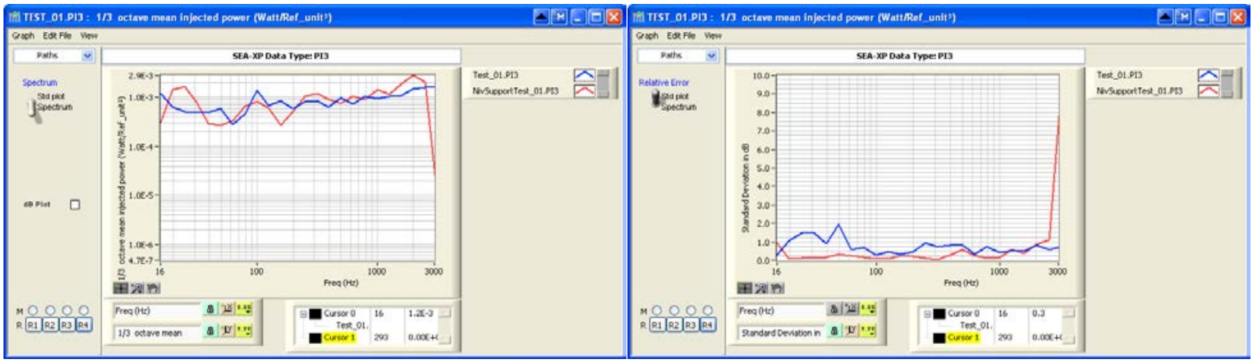

Figure 23: On left Conductances measured on free OSB (blue) and in the region supported by the resilient material (red); on right related standard deviation given in dB around the mean value

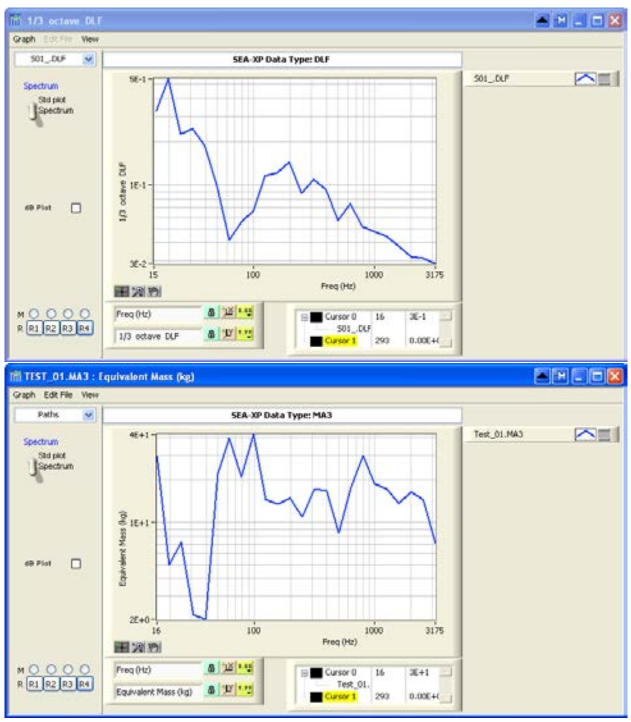

Figure 24: On left DLF of OSB 18 from PIM measurement and on right equivalent mass

2.5.2 Simulation of impact hammering on OSB18

OSB18 material properties are defined in Figure 25 with related measured and calculated conductances from SEA+ model. Agreement between measured and calculated conductances confirms the choice of OSB elastic parameters.

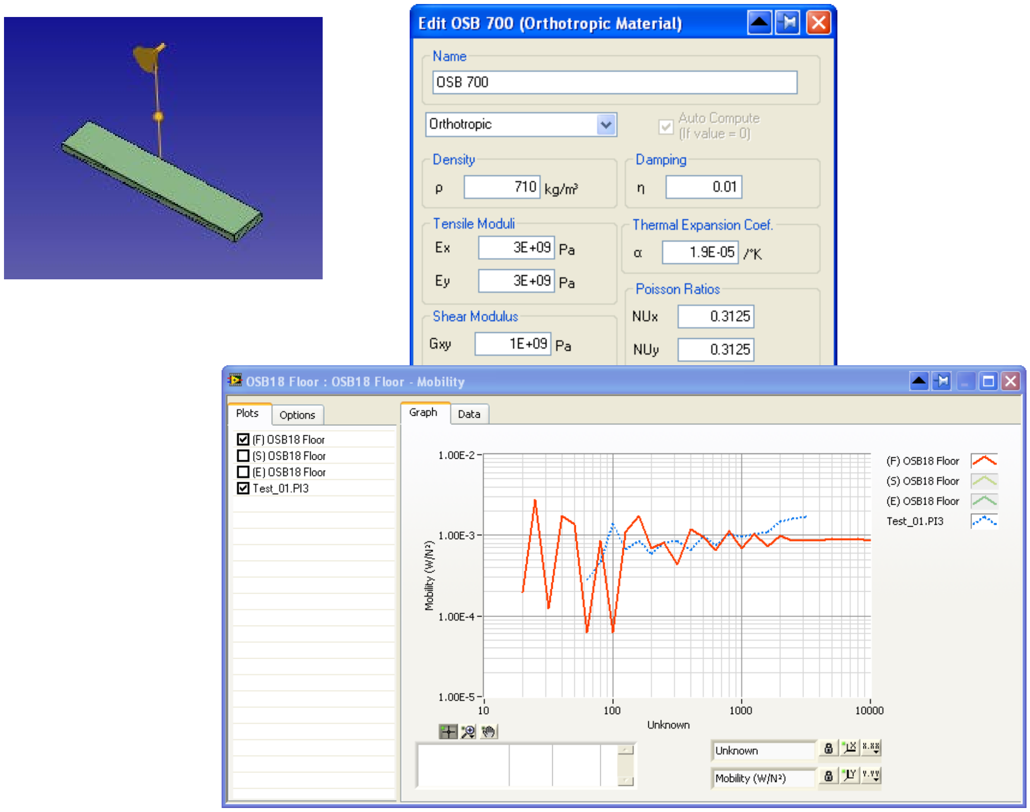

Figure 25: OSB properties on left and on right predicted and measured conductance of 18mm –OSB panel

The measured DLF is imported in the OSB subsystem and predicted rms velocity is compared to measured one (under impact hammer) in Figure 26.

Above 2kHz, the predicted response and the measured one start to deviate from each other partly due to previously observed difference in HF predicted and measured HF conductance as it can be seen by observing that the deviation between measured velocity and predicted one is larger in HF with unit force load because conductance *Y* is theoretically calculated and $Pinj = Yx\ F^2$.

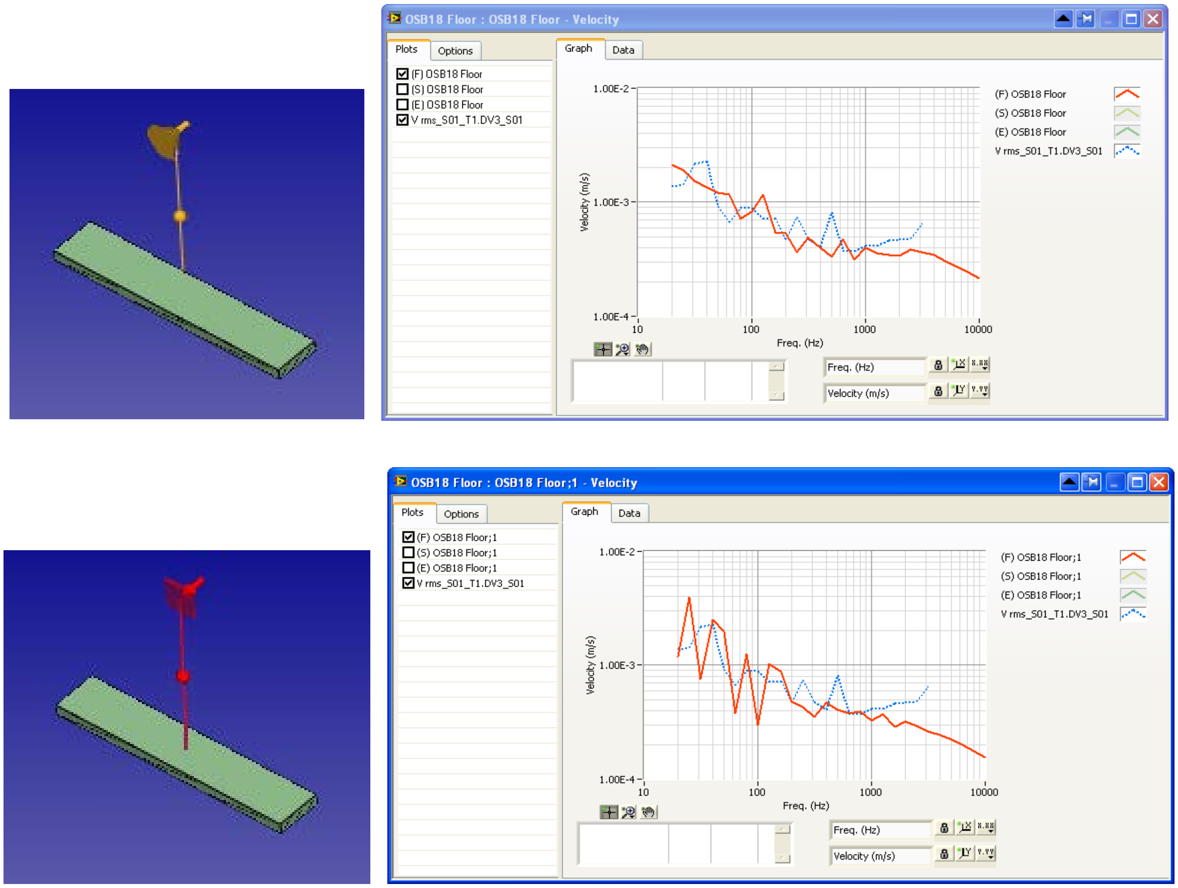

Figure 26: Top Prediction and measured mean velocity response of the OSB18 panel under measured injected power and bottom velocity response under unit force load

2.5.3 Simulation of shock machine excitation on OSB18

As done for concrete floor, the mean velocity response of the OSB floor is computed from recorded acceleration time histories at the various locations of the shock machine in operating conditions.

The mean autospectrum of acceleration is given in narrow band in Figure 27.

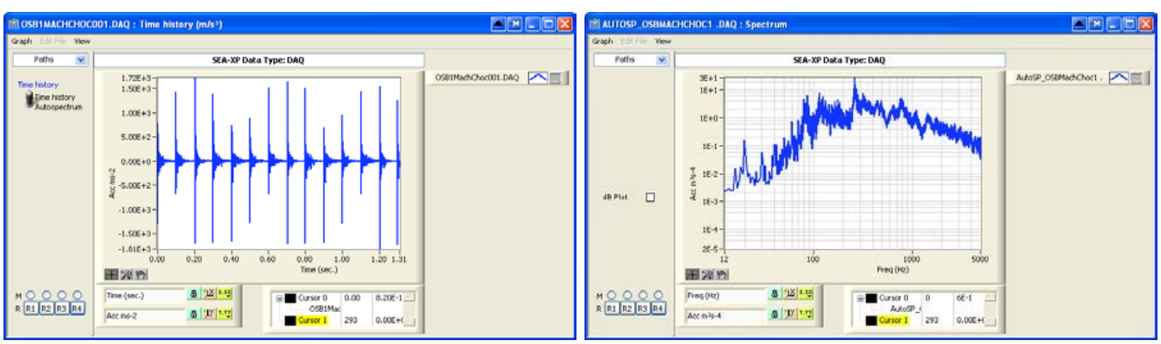

Figure 27: Left: One particular time history record of the OSB acceleration response under operating shock machine load

The mean 1/3rd octave velocity computed from previous autospectrum is given in Figure 28. The predicted response is closed to the measured one.

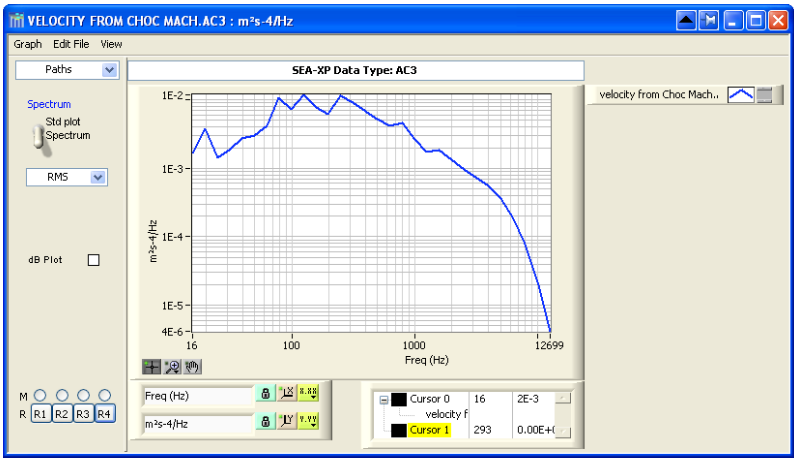

Figure 28: Mean velocity response of OSB floor under operating shock machine load

The injected power of the shock machine is then processed as:

$$P_S = P_H \frac{\langle v_S^2 \rangle}{\langle v_H^2 \rangle}$$

and the force is obtained as:

$$F^2{}_S = \frac{\langle v_S^2 \rangle}{\langle v_H^2 \rangle} \Rightarrow F = \frac{\sqrt{\langle |v_S^2| \rangle}}{\sqrt{\langle v_H^2 \rangle}} = \frac{\langle v_{S\_rms} \rangle}{\langle v_{H\_rms} \rangle} ..$$

with H for "Hammer" and S for Shock machine". The related spectra are given in Figure 29. When the equivalent force is applied to the OSB18 panel the predicted and measured mean velocity response are nearly identical (see Figure 30)

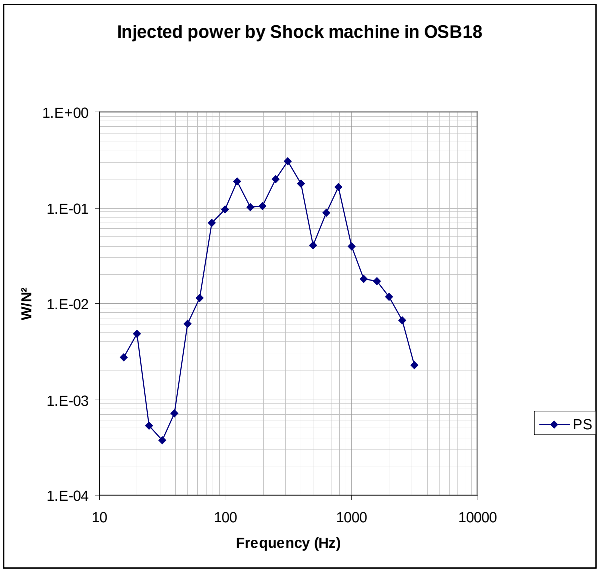

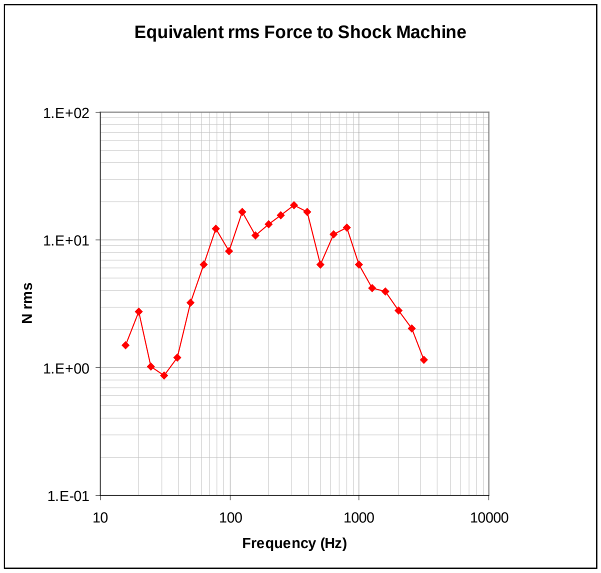

Figure 29: Righ Injected power from the shock machine in OSB18 and left related equivalent rms force

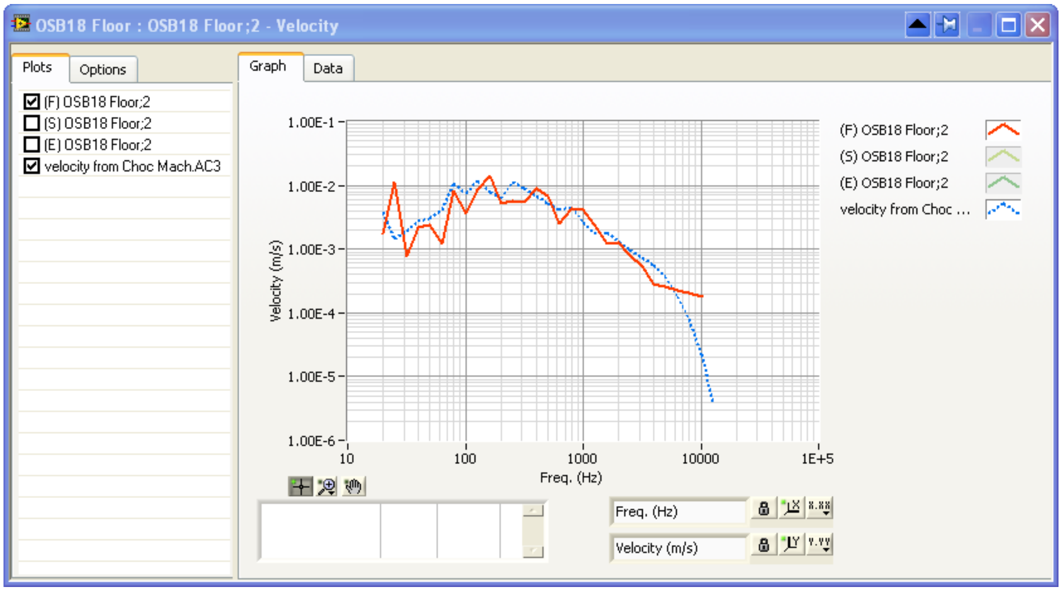

Figure 30: Predicted (red) and measured (dashed blue) mean rms velocity of the OSB18 panel under shock machine load

2.6 Comparing forces from shock machine on concrete and on OSB

The forces delivered by the shock machine are showing very different amplitudes and spectra, depending whether they are applied to concrete or to OSB floor.

The ratio of Shock machine force "Fconcrete/F_Osb" is given in Figure 31 and compared in same Figure with related ratio between measured hammer forces recorded with mid-sized hammer.

Some care needs to be taken in comparing spectra as force responses are defined in rms N and then sensitive to window length.

A quick scaling of transient events recorded with different window length is to calculate their total signal energy and to compare them. The total energy is obtained by:

$$E_{FF}(\omega,T) = T \cdot S_{FF}$$

where T is the record window length and S_{FF} the power spectral density or PSD of F.

The PSD is also equal to:

$$S_{FF} = T \cdot F^2$$

where F² is the autospectrum.

Then the total signal energy is equal to:

$$E_{FF}(\omega,T) = T^2 \cdot F^2$$

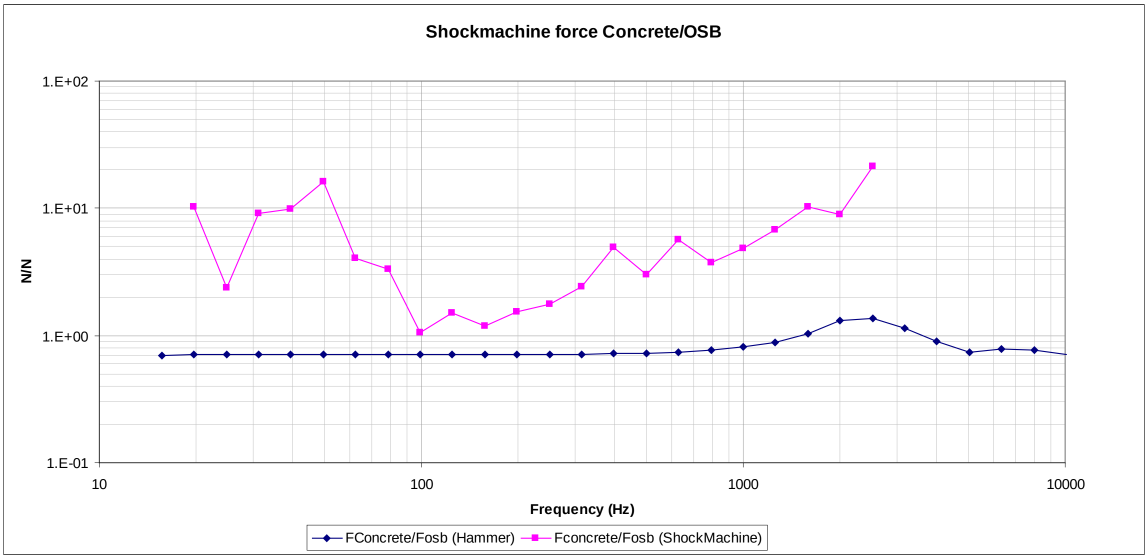

Figure 31: Ratio of force_concrete/force osb estimated in shock machine test and in impact hammer test

If we directly observe the compared force spectra applied by impact hammer and by shock machine (Figure 32 and Figure 33), we see shock machine spectrum showing larger offset compared to impact hammer when it is applied to the hard concrete (Figure 33). This offset is smaller on force applied to OSB (Figure 32) but showing a more pass-band behavior.

Comparing shock-machine impact on both OSB and concrete in Figure 34 shows the OSB impact is much less efficient in HF range due most probably to low-pass filtering of injected power as usual for soft structures.

As a conclusion, the shock machine is interacting with the floor bending stiffness. Down to 500 Hz, it may be assumed that the force is nearly independent of floor bending stiffness while this assumption does not held above 500 Hz.

As shown in this report, PIM test protocol is providing an easy way to calibrate the shock machine spectrum in order to predict reliable output levels of vibration from the SEA model.

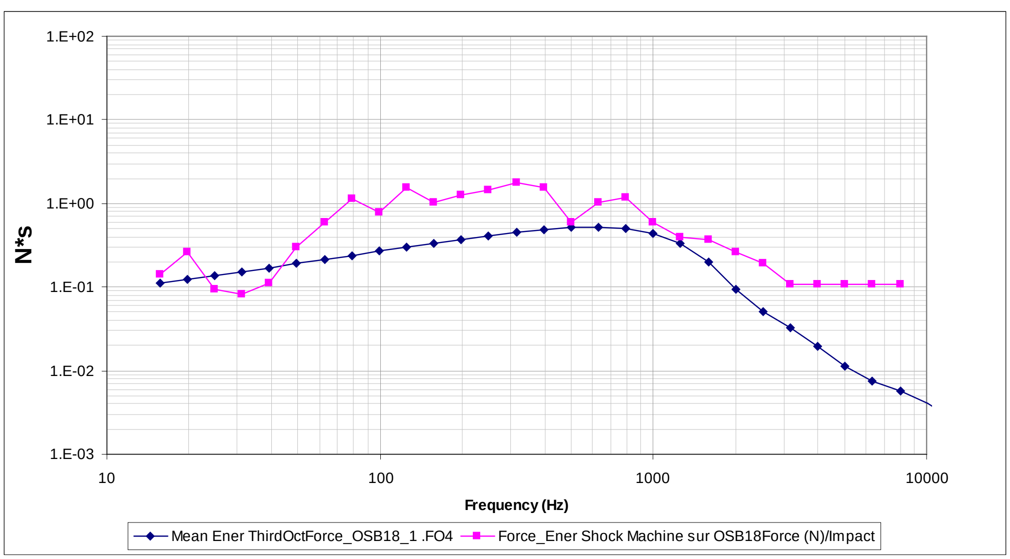

Figure 32: Rms spectrum of mean force applied by shock machine when operating on concrete floor and related rms force spectrum of mean force applied with impact hammer

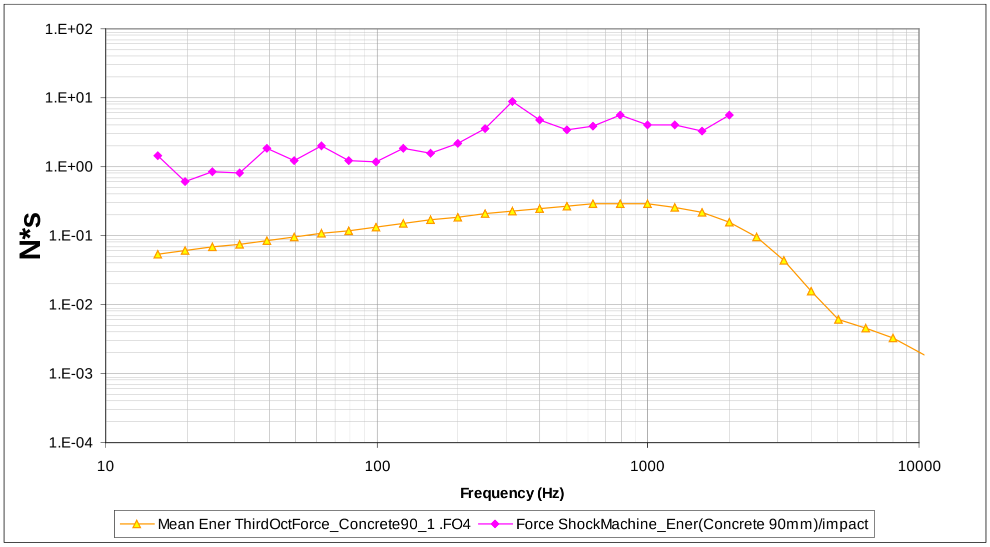

Figure 33: Rms spectrum of mean force applied by shock machine when operating on OSB floor and related force spectrum of mean force applied with impact hammer

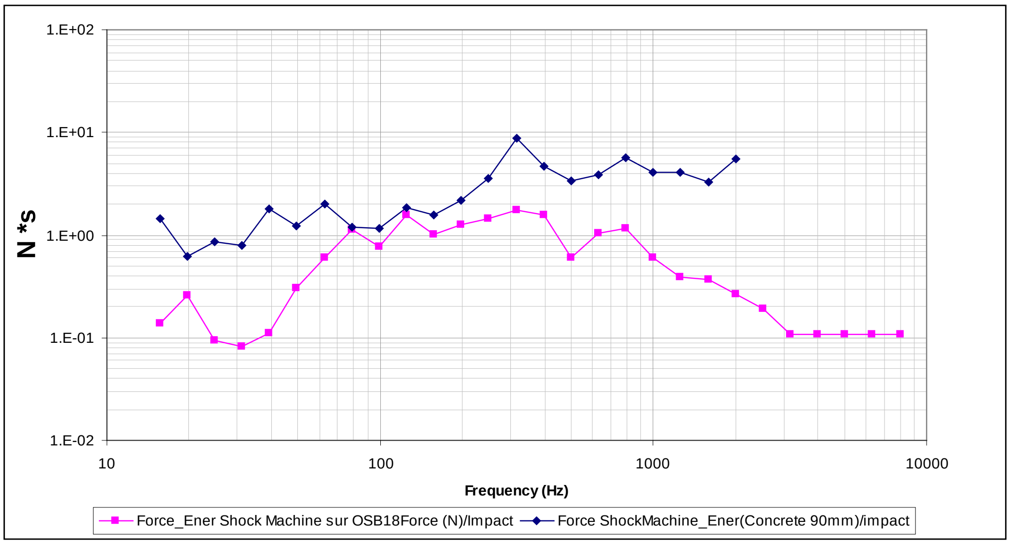

Figure 34: Compared reconstructed mean force spectra per impact applied by shock machine when operating on concrete and OSB floors

2.7 Prediction of Time history response to the shock machine

2.7.1 Brief explanations on SEA-SHOCK theory

The module SEA-Shock available in SEA+ is now used to reconstruct a time history response from the SEA model. The SEA model does not deliver any invertible transfer so to reverse the analysis to time domain, some additional signal processing is required as well as a couple of assumptions.

First of all, we need as input a force time history. Second, connected subsystem needs to be weakly coupled in order that in any subsystem, one can reconstruct a scaling function (a modal complex FRF) based only on the local dynamic response of the receiver (subsystem in which we need the time history response).

Basic theory implemented in SEA-Shock is based on the calculation of this scaling function obtained as the complex modal response to a unit-force applied in the receiver subsystem. This special FRF is providing a phase to the real-value FRF given by the classic frequency solution of the SEA network. In the receiver the real-valued FRF is made complex and the complex amplitudes given in narrow frequency bands are interpolated for satisfying the condition that their integral over the SEA frequency bands has to converge to SEA FRF modulus. This is the essence of the LMPR algorithm (Local Modal Phase Reconstruction) which provides an invertible FRF function in the complex frequency domain. Convoluted with the time history of the input, the time history of the receiver can then be synthesized.

This methodology has been developed over ten years in research applied to spacecraft to predict response to shock tests.

2.7.2 Concrete floor transient response

To perform a quick calculation with SEA-Shock, we need to define some representative force in the time domain.

The Pulse Generator function of SEA is used for that. Figure 35 shows the pulse response is fitted manually to describe the T*PSD response of the receiver. By choosing exponentially decaying sine signal, we are roughly approaching the measured T*PSD. More refined way has to be developed for better fit to exact shape of T*PSD but we can see from the T*PSD graph of the decaying sine and the T*PSD of the measurement that at least below 1000 Hz , levels from this simple force profile are similar and main peak at 500 Hz is well reproduced.

This signal is made quite impulsive with an arbitrary duration of around 10 ms.

When this input time history signal (named "Shock machine approximation") is stored in SEA+ database, it has to be allocated to a time domain source (Figure 36).

The subsystem is declared as "LMPR receiver" to output the response in the time domain after connecting the time domain source to the concrete floor (see picture in Figure 36). It is now surrounding by a transparent sphere indicating it is now the output.

Figure 37 shows the comparison between prediction and measured response. As expected from selected T*PSD force spectrum, low and mid frequencies content below 500 Hz is well reconstructed and HF are filtered as selected excitation is behaving more like a low pass filter. It is why the measured signal is filtered by a low pass of order 2 and compared with the prediction.

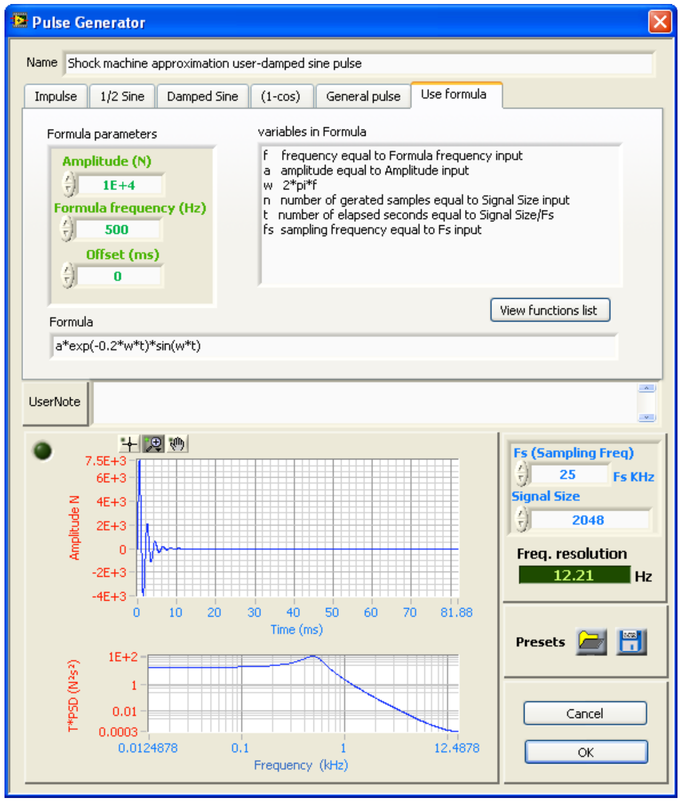

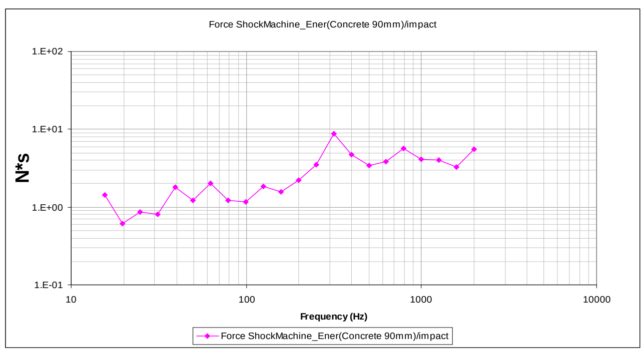

Figure 35: Pulse Generator dialog box in SEA+ and entering a formula for fitting with current force autospectrum

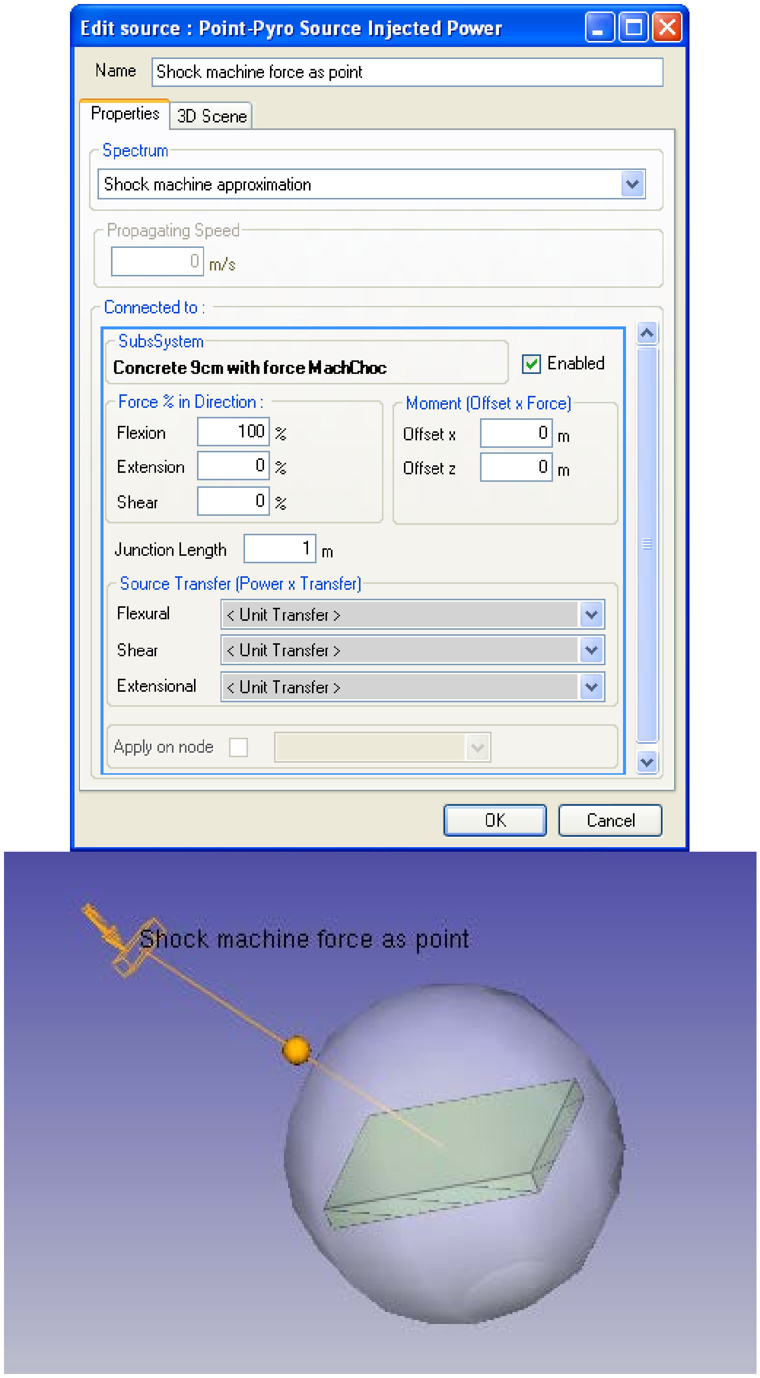

Figure 36: Setting the shock source to "Shock machine approximation"

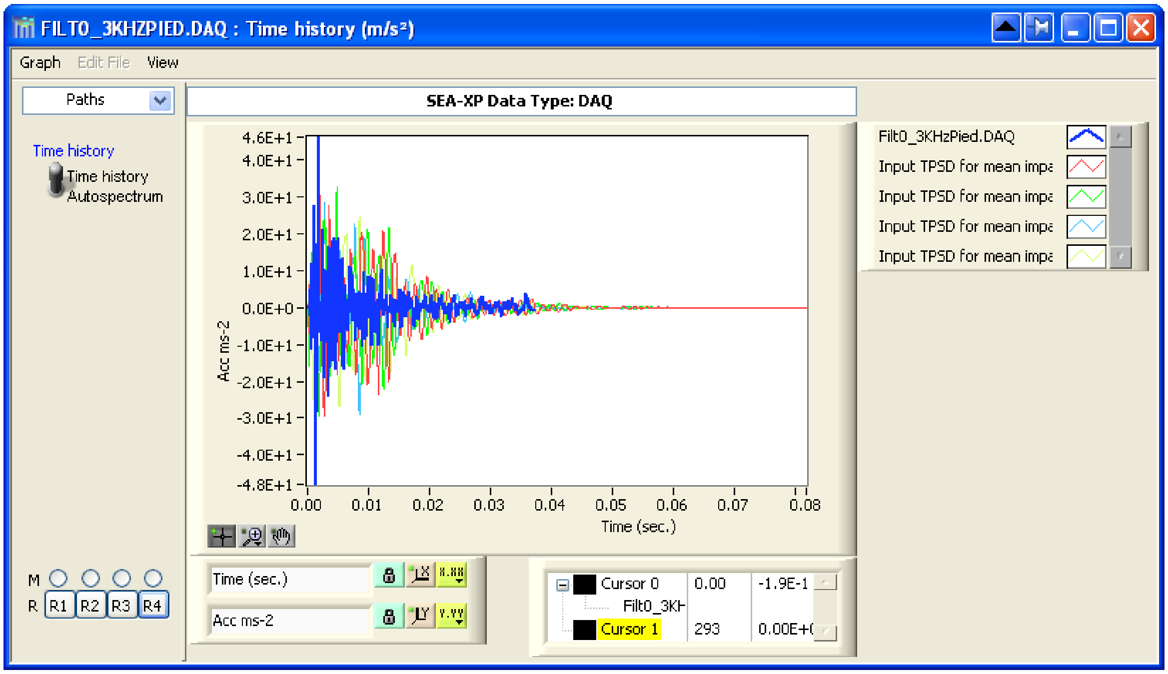

Figure 37: Synthesized and measured force pulse (blue) when impacting the concrete floor

3. Second test campaign in FCBA

3.1 Test conditions

The tests were performed in FCBA on August 31, 2015 on another wood floor. The floor was characterized by experimental SEA measurements and records of acceleration of floor under excitation by shock machine were recorded. The tested floor is seen in Figure 38.

Figure 38: Tested OSB floor 2d test campaign

This floor is made of OSB 20. Size is 4 m length and 2.5 m width with a weight 70kg corresponding to mass density of 350 kg.
The floor is supported on a network of parallel X studs lying on concrete ground. Distance between studs is 0.6 m. Individual panels of OSB are screwed every 0.3 m to studs on stud.
Elementary panels are 0.6 X 0.5 m².

3.2 ESEA measurements on OSB 20 floor

Three ICP accelerometers are fixed to the floor on OSB surface. Hammer impacts are then given at various point locations to map the vibration field of the floor. The injected power from hammer is calculated from measured force and acceleration at driving points.

Injected power is given for the three references in Figure 39. Validity frequency band lies from 50 Hz to 4 kHz. Reference 3 is given more level at low frequency as the accelerometer is near panel center while other transducers are nearer from local edges of OSB panels.

From mean FRF recorded at the various points, injected power and damping, the equivalent mass is computed (Figure 41). The evolution of equivalent mass with frequency is a pertinent indicator of how the floor is behaving: From 100 to 500 Hz the mass is decreasing down to 60-100 kg and is climbing up above 800 Hz. Above 3 kHz, mass is collapsing as limit of measurement is reached.

For 390 kg/m^3 density, OSB floor is 70 kg (without stud mass) and this is the order of magnitude in the region 500-800 Hz.

Below 500 Hz mass is larger due to added mass of studs.

Above 800 Hz, the apparent mass increase is due to floor design: coupling becomes weaker and weaker with frequency between screwed elementary OSB panels. It leads to stronger decrease of acceleration with distance that what would be expected for a continuous panel of 4x2.5 m². Equivalent mass is then increasing, meaning less velocity for a given energy than in a continuous panel.

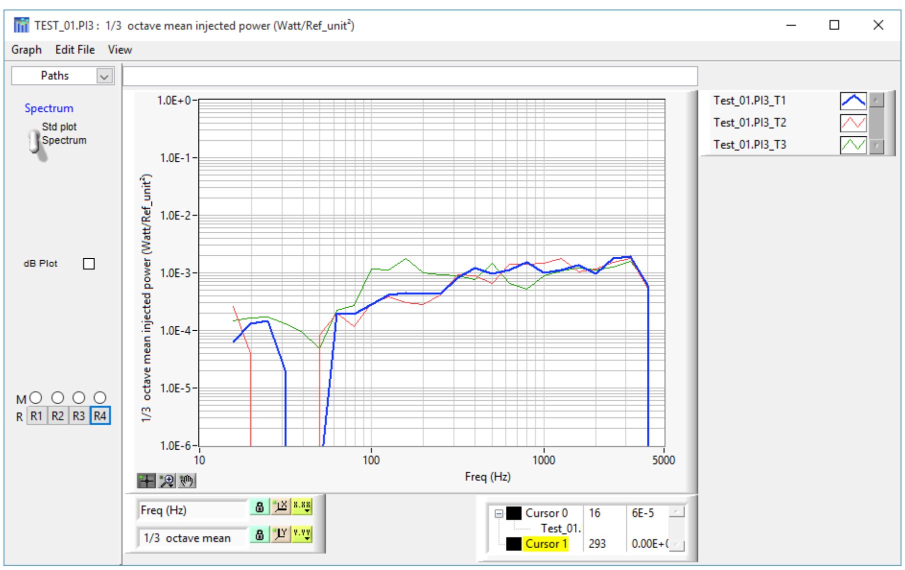

Figure 39: Injected power/N² (real part of driving point mobility) at the 3 reference nodes

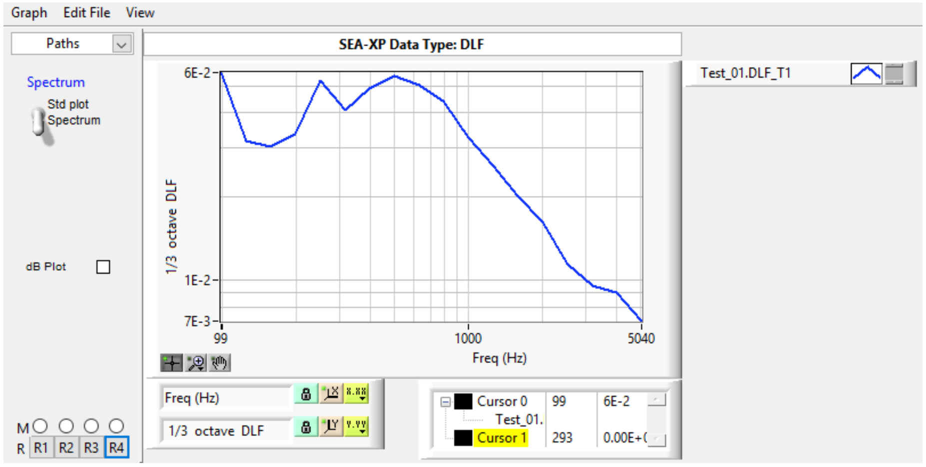

Figure 40: DLF measured by reverberation time

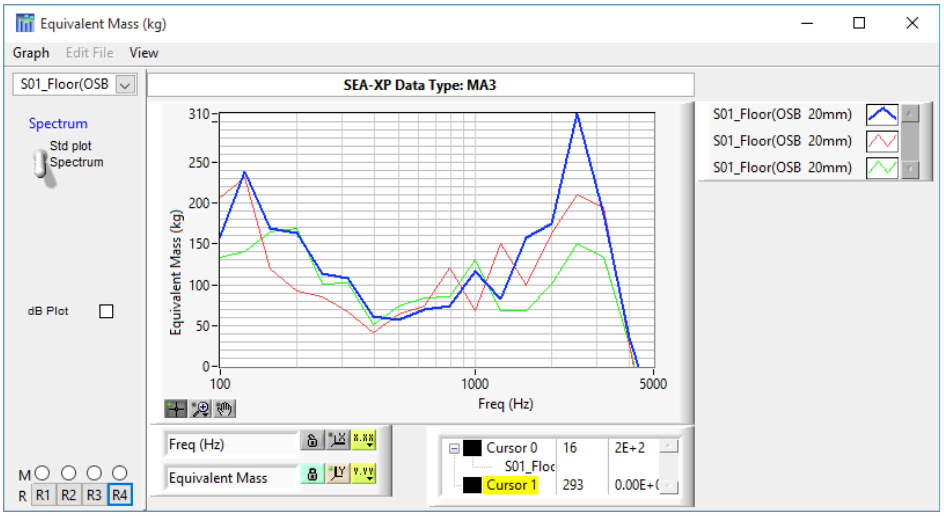

Figure 41: Equivalent mass measured by ESEA

3.3 Correlation of ESEA test on OSB 20 floor with SEA prediction

The measured driving point mobility at the three references is compared with mobility of SEA floor model.

The material properties to match with measurement are given in Figure 42. Elastic properties are falling in the range of light OSB panel known values. Better fitting is obtained with section of 18 mm and mass density of 390 kg/m^3 is calculated with this thickness. A unit-point force is applied to the SEA model of floor to simulate impact hammer excitation. The DLF of the floor is set to the measured DLF given in Figure 40. Rms velocity can be predicted within 2 dB from measurement per 1/3rd octave band with this model as shown in Figure 43.

Figure 42: Mobility measurements compared with analytical prediction (red curve) best results with here above OSB characteristics and 18 mm thickness

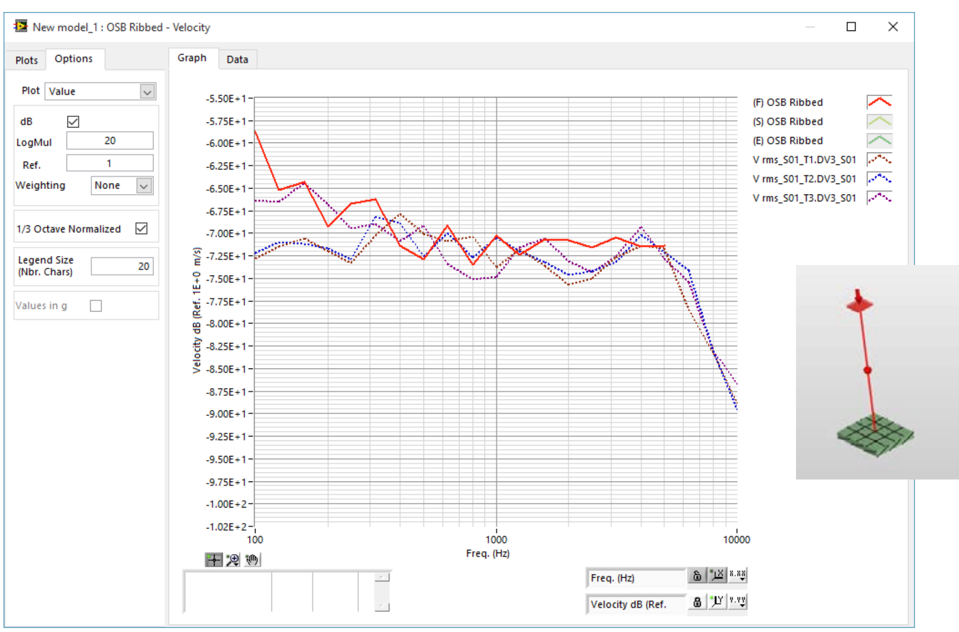

Figure 43: Measured Mean velocity of the floor for the 3 reference nodes compared with SEA floor model when using measured flexural damping in the model and a unit-force as load

3.4 Measuring acceleration with the shock machine

The three reference accelerometers are still at same location. The shock machine is moved from one sub-panel to another (23 positions, leading to 23X3 accelerations records-one sub-panel location has been skipped n°18). Recorded rms acceleration spectra integrated in 1/3rd octave band are given in Figure 44. Above 500 Hz, acceleration levels are scattered within 20 to 30 dB range, depending on shock machine-reference distance. Figure 45 shows this scattering for reference #1 with red thick line being the acceleration when shock machine is located in the sub-panel containing this reference.

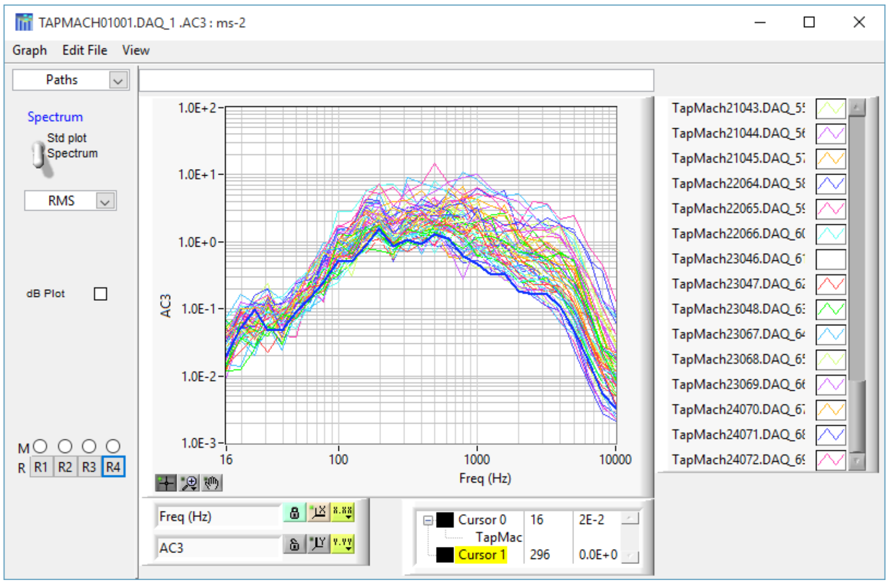

Figure 44: Measured Mean floor acceleration at the 3 references for the 23 locations of the shock machine on OSB20 floor

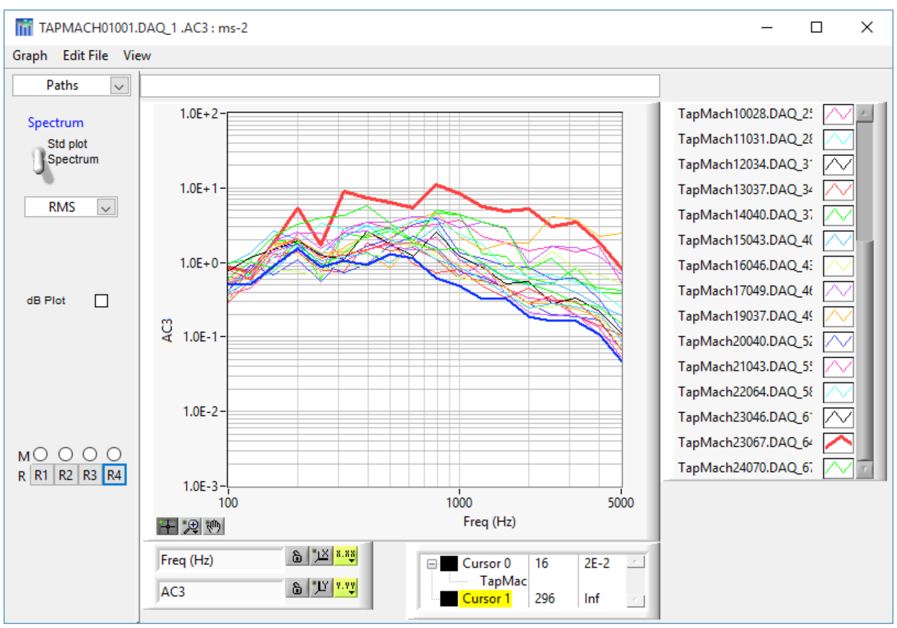

Figure 45: Measured Mean floor acceleration at reference #1 for the 23 locations of the shock machine on OSB20 floor

3.5 Predicting shock machine acceleration with SEAWOOD

3.5.1 Injected power from shock machine

The injected power from shock machine is estimated from hammer impact injected power and from shock machine acceleration.

$$P_{TM} = \langle P_{Hammer} \rangle_{ref} \cdot \frac{\langle v_{TM}^2 \rangle}{\langle v_H^2 \rangle}$$

In previous formula, injected power from hammer is averaged over the three references. Velocity² is averaged over all available records, considering the floor as a single subsystem.

Resulting shock machine injected power is given in Figure 46.

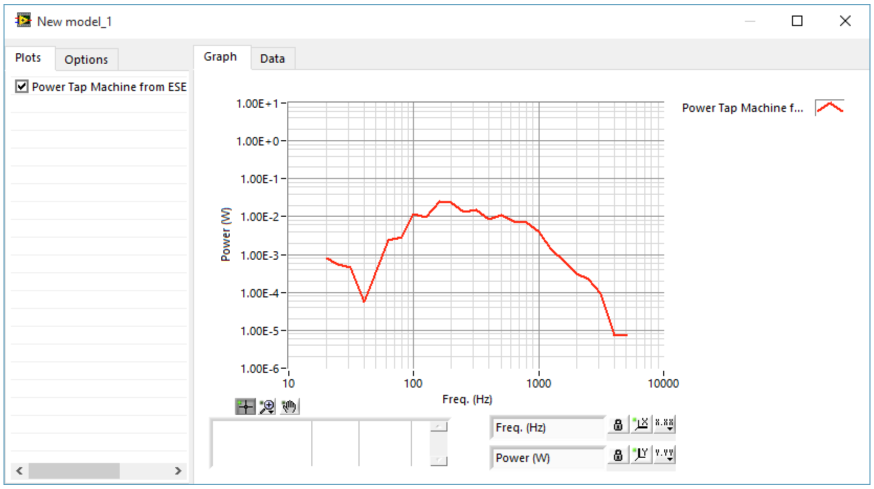

Figure 46: Injected power from shock machine estimated from hammer impact and from shock machine acceleration

3.5.2 Predicting sub-panel acceleration with SEAWOOD

A detailed model of the OSB floor is built with SEAWOOD as seen in Figure 47. All OSB sub-panels (0.5 m X 0.68 m) are cross-connected and connected to studs. A multipoint connection is assumed between panels with 0.3 m spacing between connecting points. Connected panels are either connected by pair (along x-axis) or multiport connected (2 OSB panels+ 1 stud). The damping loss factor allocated to each sub-panel is the measured ESEA DLF estimated from the floor. One shock machine location is simulated by applying the shock machine injected power to one particular sub-panel. Predicted acceleration in sub-panels is given in Figure 48. The levels are remarkably similar to recorded ones given in Figure 45.

Therefore given injected power and mean FRF velocity under impact hammer and mean floor acceleration under shock machine load, an accurate SEAWOOD model of the floor can be built from estimated shock machine injected power and floor damping, assuming some realistic model of junction between floor components.

This model is valid above first local resonances of sub-panels (i.e. 500 Hz). Below the model gives correct order of magnitude but as the floor behaves more as a single panel, acceleration in the excited subsystem tends to be over-predicted as energy is mostly concentrated in a smaller area in the model while it is actually spread over the entire floor in this low frequency range.

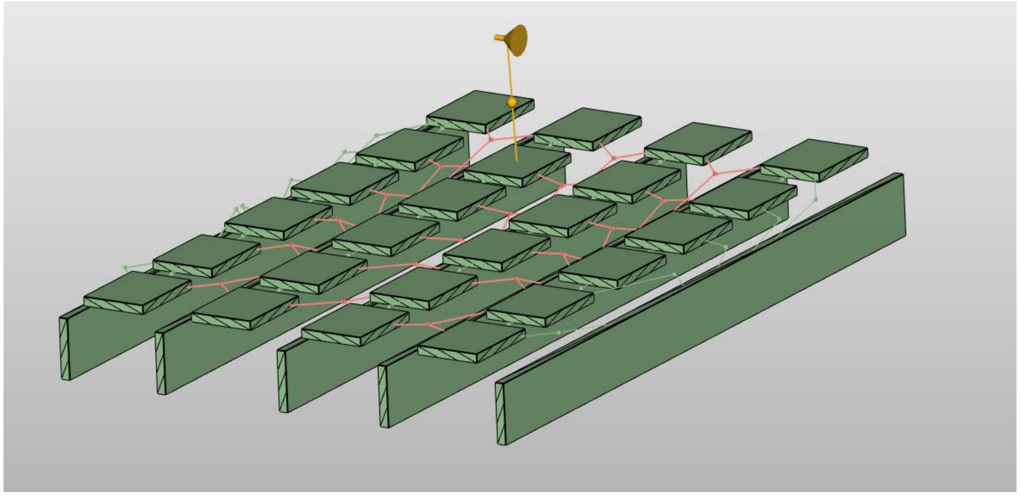

Figure 47: OSB20 floor detailed SEAWOOD model

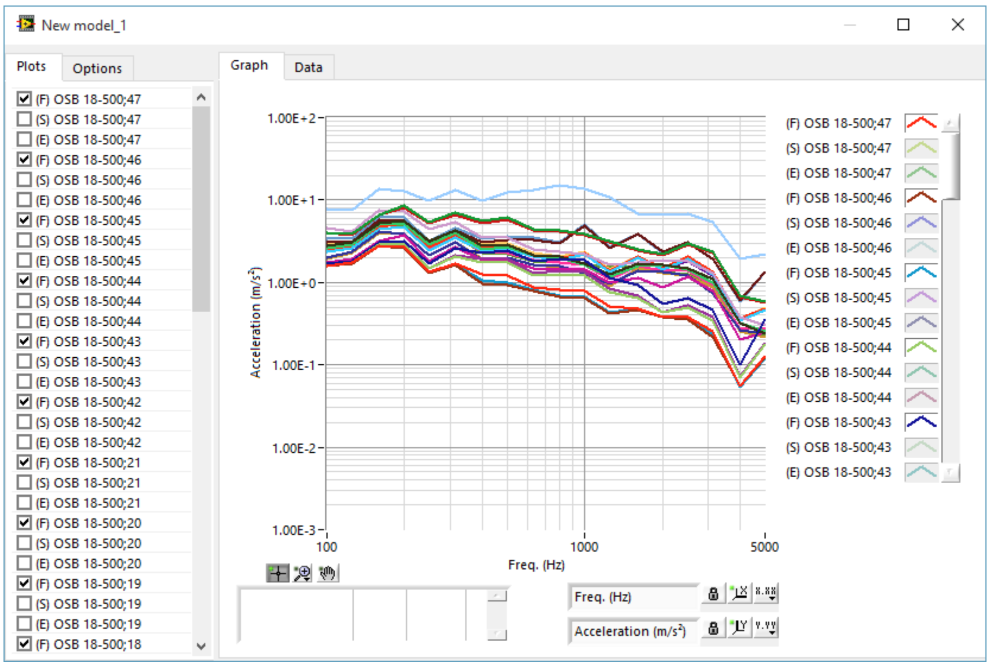

Figure 48: Predicted floor acceleration in all sub-panels for shock machine location shown in Figure 47

4. Conclusions

We have shown that a simple method based on Power Injected Method (PIM) on an isolated floor can provide the injected power spectrum of the shock machine in different analyzed cases

The injected power from the shock machine is found to be dependent on floor bending stiffness and more high frequency filtering occurs on soft floor made of OSB compared to thick floor in concrete.

The transient response time history of the floor can also be simulated by SEA-Shock module of SEAWOOD software. Regarding this time history prediction, a force input is required. Current input by force is difficult to assess with accuracy as force from shock machine was not measured in the test campaign and an existing SEA-Shock force profile was tuned to fit identified power inject spectrum inducing limitation in HF range.

In the OSB20 test case, we show that the floor mean acceleration per small sub-panels can be directly predicted in the frequency domain as rms acceleration from detailed SEAWOOD model of the floor. This method is easier to use as it does not required any force input from the shock machine.